Published in final edited form as:
Int J Cancer. 2012 May 15; 130(10): 2464–2473. doi:10.1002/ijc.26279.

Inecalcitol, an analog of 1α,25(OH)$_2$D$_3$, induces growth arrest of androgen-dependent prostate cancer cells

Ryoko Okamoto[1,*], **Remi Delansorne**[2], **Naoki Wakimoto**[1], **Ngan B. Doan**[3], **Tadayuki Akagi**[1], **Michelle Shen**[1], **Quoc H. Ho**[1], **Jonathan W. Said**[3], and **H. Phillip Koeffler**[1,4]

[1]Division of Hematology and Oncology, Cedars-Sinai Medical Center, UCLA School of Medicine, Los Angeles, CA, USA

[2]Hybrigenics, Paris, FRANCE

[3]Department of Pathology, Center of Health Science, UCLA School of Medicine, Los Angeles, CA

[4]Cancer Science Institute of Singapore and National Cancer Institute, National University of Singapore, Singapore

Abstract

19-nor-14-epi-23-yne-1,25(OH)$_2$D$_3$ (inecalcitol) is a unique vitamin D$_3$ analog. We evaluated theactivity of inecalcitol in a human prostate cancer model system. The analog was 11-fold more potent than 1,25(OH)$_2$D$_3$ in causing 50% clonal growth inhibition of androgen-sensitive human prostate cancer LNCaP cells. Inecalcitol, more than 1,25(OH)$_2$D$_3$, reduced in a dose-dependent manner the expression levels of the transcription factor ETV1 and the serine/threonine protein kinase Pim-1, both of which are up-regulated in prostate cancer. Remarkably, dose challenge experiments revealed that inecalcitol maximum tolerated dose (MTD) by intraperitoneal (i.p.) administration was 30 μg/mouse (1,300 μg/kg) three times per week, while we previously found that the MTD of 1,25(OH)$_2$D$_3$ is 0.0625 μg/mouse; therefore, inecalcitol is 480 times less hypercalcemic than 1,25(OH)$_2$D$_3$. Pharmacokinetic studies showed that plasma half-life of inecalcitol was 18.3 minutes in mice. A xenograft model of LNCaP cells was developed in immunodeficient mice treated with inecalcitol. The tumors of the diluent-treated control mice increased in size but those in the inecalcitol treatment group did not grow. Our data suggest that inecalcitol inhibits androgen-responsive prostate cancer growth *in vivo* and should be examined either alone or with other chemotherapy in clinical trials in individuals with rising serum prostate-specific antigen (PSA) after receiving either surgery or irradiation therapy with curative intent.

Keywords

Vitamin D; inecalcitol; prostate cancer; antiproliferative effects

Introduction

Prostate cancer is the most frequently diagnosed and the second leading cause of cancer mortality in males in the United States [1]. Preclinical data have shown that calcitriol [1α,25-dihydroxycholecalciferol, 1,25(OH)$_2$D$_3$] has a significant antitumor activity and may potentiate the efficacy of chemotherapy. Several mechanisms have been proposed for the antiproliferative effect of 1,25(OH)$_2$D$_3$ in prostate cancer cells, including promotion of cell

[*]Correspondence: Ryoko Okamoto, Address: 8700 Beverly Blvd, Los Angeles, CA90048, USA, Fax: +1-310-423-0225, Ryoko.okamoto@cshs.org.

cycle arrest, induction of apoptosis, and modulation of kinase pathways [2–6]. However, the precise molecular mechanism(s) associated with the antiproliferative effects of 1α, $25(OH)_2D_3$ is not fully elucidated.

Since $1,25(OH)_2D_3$ causes hypercalcemia, the dose that can be given to patients is less than the amount theoretically required for anticancer activity. Consequently, new analogs of vitamin D_3 that are potent but less calcemic, are being synthesized and tested. 19-nor-14-epi-23-yne-$1,25(OH)_2D_3$ (inecalcitol, TX-522) is a synthetic analog of vitamin D_3 that has a 14-epi modification. This compound has very little calcemic activity, but appears, nonetheless to retain potent stimulation of the vitamin D receptor (VDR) [7].

Pim kinases are cytoplasmic serine/threonine kinase's that control programmed cell death by phosphorylating substrates that regulate both apoptosis and cellular metabolism [8]. The proto-oncogene Pim-1, which is located on 6p21, is often up-regulated in its expression in leukemia and prostate cancers [9, 10]. High expression of Pim-1 is associated with genomic instability induced by disruption of the mitotic spindle checkpoints [11], and is implicated in tumorigenesis [12]. Pharmacological modulation of Pim-1 may have an impact on the treatment of prostate cancer.

Recurrent chromosomal rearrangements involving ETS transcription factors including ETS variant 1 (ETV1) are found in human prostate tumors [13]. Overexpression of either truncated or full-length ETS protein often occurs as a result of chromosomal translocation, placing the ETS gene under the control of a robust promoter [14]. However, high expression of full-length ETV1 even without chromosomal translocation, has been observed in many prostate tumors [15].

In this study, we investigated the anticancer activity of inecalcitol against prostate cancer cells *in vitro* and *in vivo* and explored its mechanism of action.

Materials and Methods

Cells and compounds

Prostate cancer (PC-3, DU145 and LNCaP) and myeloid leukemia (HL-60) cell lines were obtained from American Type Culture Collection (Manassas, VA), and they were maintained according to their recommendations. DU145 cells were grown in DMEM (Life Technologies Corp.; Carlsbad, CA) supplemented with 10% fetal bovine serum (Gemini Bio-Products; West Sacramento, CA) and 100 IU penicillin/100 μg/ml streptomycin (Life Technologies Corp.). LNCaP, PC-3, HL-60 cells were cultured in RPMI-1640 with 10% FBS and antibiotics. All cell lines were maintained in a 37°C incubator containing 5% CO_2.

High purity crystalline inecalcitol was kindly provided to us by Hybrigenics (Paris, France). The vitamin D_3 compounds were dissolved in absolute ethanol at 10^{-3} M, stored at −20°C, and protected from light. The structures of the $1,25(OH)_2D_3$ and inecalcitol are shown in Fig. 1. For *in vitro* use, dilutions were made in the same tissue culture media as those for cell culture. The maximal concentration of ethanol (diluent control) used in this study, had no effect on cell growth. For *in vivo* use, dilutions were made from the stock in either PBS or 50 % DMSO/PBS when the concentration was either less than 20 μg/mouse or over 20 μg/mouse, respectively.

Proliferation assay

For the sulforodamine B (SRB) assay, cells were plated at 1×10^3 cells/well into 96-well plates. After 16 h, the compound was added to the medium. After 120 h, the cells were fixed with 10% trichloroacetic acid (TCA) and stained with SRB (Sigma-Aldrich.; St. Louis,

MO), as described previously [16]. In addition, cells in single-cell suspension were enumerated and plated into 24-well flat-bottomed plates using a two-layer soft agar system with a total of 1×10^3 cells/well in a volume of 400 μl/well [17]. After 10–14 days of culture, colonies were counted. All experiments were done at least three times using triplicate wells per experimental point. Results are expressed as a mean percent ± S.D. of control plates containing no drugs.

Western blot analysis

Western blot was performed as described previously [18]. Antibody against Pim-1(sc-13513) was from Santa Cruz (Santa Cruz, CA); those against GAPDH (2118X) and ETV1 (ER81, ab81086) were from Cell Signaling Technology (Danvers, MA) and Abcam (Cambridge, MA), respectively. Blots were developed using the enhanced chemiluminescence kit (Thermo Fisher Scientific; Rockford, IL).

Quantitative real-time PCR (qRT-PCR)

mRNAs were purified from cells or tissues by RNeasy kit (QIAGEN Inc.; Valencia, CA) and RT-PCR was performed using ThermoScript RT-PCR Systems (Life Technologies Corp.) according to the manufacturer's protocol. qRT-PCR (iCycler, Bio-Rad; Hercules, CA) was performed using SYBR Green; and expression levels of target genes were normalized with β-actin. Fold change was calculated using the ΔΔCt method. The primers are listed in Supplemental Table 1.

Serum calcium levels *in vivo*

All animal experimental procedures were carried out in accordance with the NIH Guide for the Care and Use of Laboratory Animals and approved by Cedars-Sinai Medical Center Institutional Animal Care and Use Committee. The mice were fed with a standard laboratory diet. Initial "dose-finding" experiments utilized three male C57Bl/6J mice (The Jackson Laboratory; Bar Harbor, ME) per group. They were injected i.p. three times per week with a dose of vitamin D_3 compound diluted in either PBS or 50% DMSO/PBS (100 μl/mouse). Blood was drawn by submandibular bleeding every week, and serum calcium values were measured by spectrophotometry using a colorimetric assay kit (Cliniqa; San Marcos, CA).

Pharmacokinetics of inecalcitol in mice

Three male C57Bl/6J mice per group were injected i.p. with 1,300 μg inecalcitol/kg diluted in 50% DMSO/PBS (100 μl/mouse). Blood samples were obtained at 0, 5, 10, 20, 30, 45, 60, 90 minutes, 2, 3, 4, 6, and 8 hours after injection by retro-orbital bleeding. The mouse was immediately euthanized and dissected to obtain the liver for qRT-PCR assay of Cyp24 mRNA levels. Assay for measurement of plasma inecalcitol levels was performed with a GLP validated method by LC/MS-MS (SGS-Cephac; Saint Benoît, France) and plasma calcium levels were measured as above. The plasma half-life for the disappearance of the administered inecalcitol was estimated by determining the time for a 50% reduction from the peak increment level.

Murine xenograft studies

Male BNX nu/nu mice were purchased from Harlan Laboratories Co., Ltd (Indianapolis, IN) at 8 weeks of age. A total of 1×10^7 LNCaP cells in 100 μl of RPMI with Matrigel (Basement Membrane Matrix, High Concentration; BD Biosciences; Franklin Lakes, NJ) was injected subcutaneously into bilateral flanks of each mouse, resulting in the formation of two tumors per mouse. The mice were assigned blindly and randomly treated from the day after the cells were injected. Mice received inecalcitol (1,300 μg/kg in 100 μl of 50% DMSO/PBS, i.p., 3 times per week). Controls received only vehicle. Tumor sizes were

measured and calculated by the formula length × width × height × 0.5236, as described previously [19]. Blood was collected to measure the level of serum calcium. All mice were euthanized at the end of the study, and tumors were fixed in 10% neutral buffered formalin and embedded in paraffin (paraplast, Oxford Labware; St. Louis, MO) for histologic analysis.

Immunohistochemistry

Fixed tumors were embedded in paraffin and cut in 6 μm thick sections. For Ki-67 staining, tumor sections were deparaffinized with xylene and rehydrated through ethanol. Endogenous peroxidase activity was blocked with 3% hydrogen peroxide and heat-induced antigen retrieval was carried out in 10 mM citrate buffer. Antibody against human Ki-67 mAb (Dako; Glostrup, Denmark) was used and detected by diaminobenzidine staining with hematoxylin counterstaining. For terminal deoxynucleotidyl transferase dUTP nick end labeling (TUNEL) apoptosis staining, In Situ Apoptosis Kit (Millipore; Billerica, MA) was used according to the manufacturer's protocol.

Statistical analysis

For *in vitro* and *in vivo* studies, we evaluated the statistical significance of differences between two groups by two-tailed Student's t-test and two-way ANOVA. Asterisks shown in figures indicate significant differences of experimental groups in comparison (*$p<0.05$, ** $p<0.01$, *** $p<0.001$). Data points in figures represent the means ± SD (standard deviation).

Results

Growth inhibition by vitamin D_3 compounds

We studied the vitamin D_3 analog, 19-nor-14-epi-23-yne-1,25$(OH)_2D_3$ (inecalcitol, TX-522) that has a 14-epi modification, as well as 1,25$(OH)_2D_3$ (Fig. 1Aa). Their abilities to inhibit the growth of human prostate cancer cell lines (PC-3, DU145, LNCaP) and a human myeloid leukemia cell line (HL-60) were examined by SRB and clonogenic assays. Cells were plated in the presence of vitamin D_3 compounds at 10^{-12} to 10^{-6} M and cultured either for 120 h for the SRB assay or 10–14 days for the clonogenic assay. Dose-response curves were drawn (Figs. 1Ab and Ac), and the dose that inhibited 50% cell growth [effective dose (ED_{50})] was determined (Supplemental Table 2). SRB assay in liquid culture showed that the ED_{50} of inecalcitol was 2.1×10^{-9} M for the androgen-dependent LNCaP prostate cancer cells. The compounds slightly inhibited the growth of PC-3 and DU145 cells (Fig. 1Ab). Clonogenic soft agar assays of LNCaP and HL-60 cells showed that ED_{50}s of inecalcitol were 4.0×10^{-9} M and 2.8×10^{-10} M, respectively, compared with 4.4×10^{-8} M and 3.2×10^{-9} M, respectively for 1,25$(OH)_2D_3$. Therefore, inecalcitol was about 11-fold more potent than 1,25$(OH)_2D_3$ in clonogenic assay (Supplemental Table 2).

Modulation of expression of prostate cancer-related genes by inecalcitol

Pim-1, a serine/threonine protein kinase, plays an important role in signal transduction, proliferation, and survival; and it has been implicated in haematopoietic malignancies and prostate carcinomas [10]. LNCaP prostate cancer cells express Pim-1; and therefore, we investigated the ability of vitamin D_3 compounds to modulate expression of Pim-1 protein and mRNA. Treatment of LNCaP cells with inecalcitol for 48 h resulted in decreased expression of both protein and mRNA of Pim-1 in a dose-dependent manner (Figs. 2Aa and Ab).

ETS proteins are often highly expressed in prostate cancers [20]. For example, full-length of *ETV1* is translocated to the last intron of *MIPOL1* resulting in constitutively high expression

of ETV1 in LNCaP cells [21]. Remarkably, exposure of LNCaP cells to inecalcitol (10^{-10} M - 10^{-8} M, 48 h) decreased ETV1 expression levels in a dose-dependent manner (Fig. 2 Ba). Forced expression of human ETV1 in LNCaP cells partially suppressed the growth inhibitory activity of the vitamin D_3 compounds (Supplemental text and Figs. 1S Ba and Bb).

Cyp24A1 (Cyp24) hydroxylates $1,25(OH)_2D_3$ on C-24 resulting in its inactivation. This represents a feedback homeostasis because Cyp24 expression is regulated by $1,25(OH)_2D_3$. The *Cyp24* gene has a VDR binding site within its promoter region. Inecalcitol (10^{-8} M, 48 h) was 7-fold more potent than $1,25(OH)_2D_3$ in up-regulating the Cyp24 mRNA levels (Fig. 2Bb).

Similarly, the levels of these three genes were compared in the LNCaP, PC-3 and DU145 prostate cancer cell lines exposed to the vitamin D_3 compounds. Pim-1 mRNA was detected in all three cell lines, with DU145 cells expressing 8-fold more Pim-1 mRNA than LNCaP cells (Fig. 2Ca). Vitamin D_3 compounds suppressed the Pim-1 expression levels in LNCaP and DU145 cells, but not in PC-3 cells. Level of ETV1 was 200–fold higher in PC-3 cells compared to LNCaP cells (Fig. 2Cb). ETV1 was not detectable in DU145 cells. ETV1 levels decreased in the LNCaP cells, but not in the PC-3 cells, after exposure to the vitamin D_3 compounds. Cyp24 mRNA levels increased after treatment with vitamin D_3 compounds in LNCaP, PC-3 and especially DU145 cells (Fig. 2Cc).

In general CCAAT/enhancer-binding protein (C/EBP) family of transcription factors help mediating differentiation and modulate proliferation. The family consists of 5 members. We previously reported that C/EBPδ is induced by $1,25(OH)_2D_3$ in LNCaP cells [22]. Here, we note that expression of C/EBPδ was stimulated 2-fold more by inecalcitol (10^{-10} M, 48 h) compared to a similar concentration of $1,25(OH)_2D_3$ (Fig. 2S).

Determination of maximal tolerated dose of inecalcitol

Hypercalcemia is the major toxicity of vitamin D_3 compounds. We examined the calcemic effects of inecalcitol *in vivo*. We have previously determined that the maximal tolerated dose (MTD) of $1,25(OH)_2D_3$ in mice is 0.0625 μg/mouse when given i.p. three times per week [18]. With this prior knowledge, we determined the MTD of inecalcitol. Because the dose-limiting toxicity is hypercalcemic, the serum calcium levels were monitored. Serum specimens were taken 48 h after the 3rd injection. Mice receiving 0.0625 μg/mouse of $1,25(OH)_2D_3$ had serum calcium levels close to the normal range (8.5–10.5 mg/dl). A dose of 2.5 to 20 μg inecalcitol/mouse (i.p., 3 times/week) did not cause hypercalcemia over a 10 week period (Fig. 3S Aa). In contrast, mice receiving 100 μg/mouse of inecalcitol (3 times/week) for 1 week showed hypercalcemia (Fig. 3S Aa). To examine the effect of administration of inecalcitol between 20 and 100 μg/mouse, we performed an additional experiment using doses of 20, 30, 35 and 40 μg/mouse (Fig. 3A). The mice receiving inecalcitol at 30 μg/mouse maintained their serum calcium levels within the normal range (under 10.5 mg/dl) (Fig. 3Aa). Hypercalcemia was detected in the mice treated with > 35 μg/mouse of inecalcitol after 2 weeks of injections. No significant weight loss was detected (Fig. 3Ab). Therefore, the MTD of inecalcitol by i.p. was 30 μg/mouse (1,300 μg/kg), which was 480 times less hypercalcemic *in vivo* than $1,25(OH)_2D_3$ (MTD of inecalcitol/MTD of $1,25(OH)_2D_3$: 30/0.0625). For further analysis, we performed pharmacokinetics assay of 1,300 μg/kg i.p. of inecalcitol. Peak plasma levels of inecalcitol occurred 5 minutes after injection, with a return to baseline within 60 minutes. The half-life of plasma inecalcitol was 18.3 minutes (Fig. 3Ba). Expression levels of mCyp24 mRNA in the murine livers mirrored, in delayed fashion, the serum vitamin D_3 compound levels. They were up-regulated by 180 minutes and returned to nearly undetectable levels by 500 minutes after the initial i.p.

injection (Fig. 3Bb). Overall, the plasma calcium levels remained in the normal range (data not shown).

Effect of administration of inecalcitol on the proliferation of human prostate cancer cells growing in a murine xenograft model

Next, we examined whether inecalcitol could suppress the growth of human prostate LNCaP tumor xenografts *in vivo*. Human LNCaP prostate cancer cells were inoculated into the flanks of BNX mice, followed by inecalcitol administration (26 μg/20g mouse = 1,300 μg/kg, i.p., 3 times/week). The experiment ended on day 42 due to large tumor size in the diluent-treated control group. Growth of the tumors was inhibited in the mice treated with inecalcitol alone (117.5±28.9 mm^3) compared with the growth of tumors in control mice (217.7 ±173.3 mm^3) (Fig. 4Aa). The mean tumor weight was reduced by 50 % in the group that received inecalcitol (0.13±0.06 g) compared with vehicle controls (0.26±0.13 g) (Fig. 4Ab). None of the treated mice had symptoms of hypercalcemia (Fig. 4S A), nor any significant weight loss (Fig. 4S B) nor other drug-related toxicity (data not shown). Notably, the LNCaP tumors in the control group were very vascular (Fig. 4Ba). The vascularity was inhibited in the inecalcitol treated mice (Figs. 4Ba and Bb). Ki67 positive (proliferating) cells were detected at a frequency of 50% in the control tumors compared to 26% in the inecalcitol treatment tumors(Fig. 4Bc). Likewise, the proportion of TUNEL-positive, apoptotic cells in the control group was less than 2% compared to 34% in the inecalcitol group (Figs. 4Bd). Pim-1 expression examined by qRT-PCR in the tumors at autopsy showed that treatment by inecalcitol significantly inhibited the Pim-1 expression (47%, p=0.038) (Fig. 4Ca). ETV1 expression in the tumors was also downregulated by inecalcitol treatment (84%, p=0.019) (Fig. 4Cb).

Discussion

Inecalcitol had a greater activity than $1,25(OH)_2D_3$ *in vitro* in suppressing the proliferation of human LNCaP prostate cancer cells (Fig. 1Ab). We have treated LNCaP xenografts using $1,25(OH)_2D_3$ in one of our previous studies [23]. Mice receiving the MTD of $1,25(OH)_2D_3$ (0.0625 μg/mouse/3 times a week) developed tumors as large as in the diluent control group at the end of treatment, despite showing an initial suppression of tumor growth [23]. Another study showed that $1,25(OH)_2D_3$ (5 μg/kg/2d) did not inhibit breast cancer growth *in vivo*, although the dose did not cause side-effects including hypercalcemia [7]. Therefore, many investigators have synthesized structural analogs of $1,25(OH)_2D_3$ that produced decreased hypercalcemic effects with increased potency against tumor cells *in vivo*. Inecalcitol (30 μg/mouse/3 times a week) can be given at a higher dose than $1,25(OH)_2D_3$ *in vivo* because it causes less hypercalemia. In contrast, we found that inecalcitol was 11-fold more active than $1,25(OH)_2D_3$ at inhibiting growth of LNCaP cells *in vitro*. Taken together, inecalcitol has both less hypercalcemic and greater antiproliferative activity than $1,25(OH)_2D_3$.

A study showed that inecalcitol has a lower affinity for VDR than $1,25(OH)_2D_3$, even though it has greater ability to enhanced transactivation of target genes by the VDR-RXR complex than $1,25(OH)_2D_3$ [24]. Subsequent studies have suggested that inecalcitol may achieve its enhanced activity byaltering the vitamin D receptor allowing it to bind more strongly to co-activator proteins [25]. Furthermore, almost all active vitamin D_3 analogs have decreased binding to vitamin D binding proteins [26]. This allows easier entrance into cells than $1,25(OH)_2D_3$.

The only major toxicity of $1,25(OH)_2D_3$ is hypercalcemia. A prior study [7] showed that inecalcitol had reduced calcemic activity compared to $1,25(OH)_2D_3$ in mice. They found that inecalcitol had a MTD of 80 μg/kg/every 2 days. The present study extended those findings and discovered that 1,300 μg/kg of high purity inecalcitol could be given three

times per week with no toxicity (Fig. 3); and therefore, the MTD for this analog was 480-fold greater than $1,25(OH)_2D_3$. Mechanism of the less calcemic effect of inecalcitol *in vivo* is not fully known. Pharmacokinetic assays showed that plasma half-life of inecalcitol in mice was 18.3 minutes (Figs. 3Ba). Muindi *et al.*[27] determined that the plasma half-life of $1,25(OH)_2D_3$ was around 4 h in normal mice after i.p. injections. Also, various studies calculated the plasma half-life of $1,25(OH)_2D_3$ in humans ranging from 5 to 8 h [28]. Active vitamin D_3 controls calcium absorption from the gastrointestinal (GI) tract into the body. This shorter half-life suggests that inecalcitol has less opportunity to cause GI absorption of calcium.

Metabolism of vitamin D_3 compounds occurs mainly through Cyp24. Cyp24 has a vitamin D response element within the promoter region. This represents a feedback control mechanism inactivating the biologic effects of $1,25(OH)_2D_3$ by hydroxylating it to an inactive metabolite, $1,24,25(OH)_3D_3$. After inecalcitol injection, plasma inecalcitol peaked within 5 minutes (Fig. 3Ba) and Cyp24 mRNAlevels peaked at 4 h in the murine liver (Fig. 3Bb). We found that all three cell lines increased their levels of Cyp24 mRNA after exposure to either $1,25(OH)_2D_3$ or inecalcitol (Fig. 2Cc). This suggests that the proximal pathway of action of vitamin D_3 compounds is intact in these cells, such as entry into the nucleus, as well as binding and activating the vitamin D receptor to transactivate genes. This is in contrast to the relative refractoriness of PC-3 and DU145 to growth inhibition by the vitamin D_3 compounds. Further genomic changes in PC-3 and DU145 appear to override the antiproliferative activity of vitamin D_3 compounds. Likewise, we suspect epigenetic modifications may be important in determining which genes are responsive to vitamin D hormonal control, since histone modification patterns at VDRE on promoters of vitamin D target genes and miRNAs show striking variability [29].

Pim kinases phosphorylate substrates that are involved in apoptosis and metabolism. Activated Pim-1 enhances the activity of proteins that stimulate the cell cycle, as well as enhance phosphorylated levels of the cell cycle inhibitors such as $p21^{Waf}$ [30,31,32]. The overexpression of Pim-1 induces genomic instability; furthermore, Pim-1 represses androgen receptor activity in prostate cancer cells *in vitro* [11]. Inecalcitol, more potently than $1,25(OH)_2D_3$, decreased expression of Pim-1 in LNCaP prostate cancer cells (Fig. 2). Moreover, inecalcitol inhibited Pim-1 expression levels in LNCaP tumors growing *in vivo* (Fig. 4Ca). Therefore, the data showed that inecalcitol modulates levels of Pim-1 in LNCaP cells, which may account for some of the anti-proliferative properties of vitamin D_3 compounds.

Full-length *ETV1* is integrated into the last intron (intron 13) of *MIPOL1* gene at 14q13.3–14q21.1 in LNCaP cells, and it is highly expressed in these cells [15, 21]. Genes (SLC25A21, MIPOL1, FOXA1 and TTC6) at the region of the breakpoint are suggested to be overexpressed in prostate cancer [21]. Exposure of LNCaP cells to inecalcitol (10^{-8} M, 48 h) decreased ETV1 expression levels by 88% (Figs. 2Ba and Cb). In contrast, expression of ETV1 in PC-3 cells is under the control of its endogenous promoter; and to our knowledge, *ETV1* gene has not been reported to be rearranged in PC-3 cells [21]. In contrast, ETV1 mRNA was expressed at greater than 200-fold in the PC-3 cells compared to levels in the LNCaP cells (Fig. 2Cb). Also, we detected full-length ETV1 protein in PC-3 cells by immunoblotting (Fig. 1S A). Levels of ETV1 in PC-3 cells were not modulated by vitamin D_3 compounds suggesting that the translocated full-length ETV1 in the LNCaP cells, but not the ETV1 promoter itself in the PC-3 cells, is inhibited by the vitamin D_3 compounds (Figs. 2Cb). Taken together, in a subset of prostate cancers, ETV1 is either a highly expressed fusion transcript with many different partners or an overexpressed full length ETV1 as a result of promoter swapping [14]. Thus, vitamin D_3 compounds might be effective in patients with these alterations.

Of note, vascularity surrounding and in the prostate tumors was markedly decreased after the inecalcitol treatment (Fig. 4Ba). Also, the proportions of Ki67 positive cells and TUNEL positive cells showed that proliferation was markedly decreased, and apoptosis was prominently increased in human prostate tumors present in the inecalcitol-treated mice (Figs. 4Bb, Bc and Bd).

Our data show that inecalcitol inhibits androgen-responsive LNCaP prostate cancer growth *in vitro* and *in vivo*, and a dose of 1,300 μg/kg, 3 times per week of inecalcitol has no demonstrable toxicity in the mice. Therefore, inecalcitol should be examined for clinical applications such as in individuals with a rising serum PSA after receiving surgery or radiation with curative intent or in those patients who require chemotherapy.

Supplementary Material

Refer to Web version on PubMed Central for supplementary material.

Acknowledgments

We thank members of our laboratory for helpful discussions. The authors, except H.P.K. and R.D., declare that there is no conflict of interest; H. P. K. consults for Hybrigenics and R.D. owns stock in Hybrigenics. We thank Dr. Charles L. Sawyers (Department of Medicine, Memorial Sloan-Kettering Cancer Center, New York, NY) for providing pMSCV-puro-human ETV1 vector. This work was supported by NIH grants (2R01 CA026038-32) (U54 CA143930-01), SWLF, the Tom Collier Memorial Regatta Foundation, Parker Hughes Fund, as well as, A*STAR of Singapore. H. P. K. is the holder of the Mark Goodson endowed Chair in Oncology Research and is a member of the Jonsson Cancer Center and the Molecular Biology Institute, UCLA. The study is dedicated to David Golde, who was a mentor and friend.

Abbreviations

C/EBPδ	CCAAT/enhancer-binding protein delta
Cyp24	Cyp24A1
ED_{50}	effective dose to inhibit 50% cell growth
ETV1	ETS (E-twenty six) variant 1
GI	gastrointestinal
inecalcitol or TX-522	19-nor-14-epi-23-yne-1,25$(OH)_2D_3$
LC	liquid chromatography
MS-MS	tandem mass spectrometry
MTD	maximal tolerated dose
PSA	prostate-specific antigen
SRB	sulforodamine B
TCA	trichloroacetic acid
VDR	vitamin D receptors
1,25$(OH)_2D_3$	1α,25-dihydroxycholecalciferol
19-nor	removal of C-19

References

1. Jemal A, Ward E, Thun M. Declining death rates reflect progress against cancer. PLoS One. 2010; 5:e9584. [PubMed: 20231893]

2. Guzey M, Kitada S, Reed J. Apoptosis induction by 1alpha,25-dihydroxyvitamin D3 in prostate cancer. Mol Cancer Ther. 2002; 1:667–77. [PubMed: 12479363]
3. Bao B, Hu Y, Ting H, Lee Y. Androgen signaling is required for the vitamin D-mediated growth inhibition in human prostate cancer cells. Oncogene. 2004; 23:3350–60. [PubMed: 15048085]
4. Yang E, Burnstein K. Vitamin D inhibits G1 to S progression in LNCaP prostate cancer cells through p27Kip1 stabilization and Cdk2 mislocalization to the cytoplasm. J Biol Chem. 2003; 278:46862–8. [PubMed: 12954644]
5. Polek T, Stewart L, Ryu E, Cohen M, Allegretto E, Weigel N. p53 Is required for 1,25-dihydroxyvitamin D3-induced G0 arrest but is not required for G1 accumulation or apoptosis of LNCaP prostate cancer cells. Endocrinology. 2003; 144:50–60. [PubMed: 12488329]
6. Nonn L, Peng L, Feldman D, Peehl D. Inhibition of p38 by vitamin D reduces interleukin-6 production in normal prostate cells via mitogen-activated protein kinase phosphatase 5: implications for prostate cancer prevention by vitamin D. Cancer Res. 2006; 66:4516–24. [PubMed: 16618780]
7. Verlinden L, Verstuyf A, Van Camp M, Marcelis S, Sabbe K, Zhao X, De Clercq P, Vandewalle M, Bouillon R. Two novel 14-Epi-analogues of 1,25-dihydroxyvitamin D3 inhibit the growth of human breast cancer cells in vitro and in vivo. Cancer Res. 2000; 60:2673–9. [PubMed: 10825140]
8. Amaravadi R, Thompson CB. The survival kinases Akt and Pim as potential pharmacological targets. Journal of Clinical Investigation. 2005; 115:2618–24. [PubMed: 16200194]
9. Dhanasekaran S, Barrette T, Ghosh D, Shah R, Varambally S, Kurachi K, Pienta K, Rubin M, Chinnaiyan A. Delineation of prognostic biomarkers in prostate cancer. Nature. 2001; 412:822–6. [PubMed: 11518967]
10. Shah N, Pang B, Yeoh K, Thorn S, Chen C, Lilly M, Salto-Tellez M. Potential roles for the PIM1 kinase in human cancer - a molecular and therapeutic appraisal. Eur J Cancer. 2008; 44:2144–51. [PubMed: 18715779]
11. Roh M, Gary B, Song C, Said-Al-Naief N, Tousson A, Kraft A, Eltoum I, Abdulkadir S. Overexpression of the oncogenic kinase Pim-1 leads to genomic instability. Cancer Res. 2003; 63:8079–84. [PubMed: 14678956]
12. Roh M, Franco O, Hayward S, van der Meer R, Abdulkadir S. A role for polyploidy in the tumorigenicity of Pim-1-expressing human prostate and mammary epithelial cells. PLoS One. 2008; 3:e2572. [PubMed: 18596907]
13. Kumar-Sinha C, Tomlins S, Chinnaiyan A. Recurrent gene fusions in prostate cancer. Nat Rev Cancer. 2008; 8:497–511. [PubMed: 18563191]
14. Gasi D, van der Korput HA, Douben HC, de Klein A, de Ridder CM, van Weerden WM, Trapman J. Overexpression of Full-Length ETV1 Transcripts in Clinical Prostate Cancer Due to Gene Translocation. PLoS One. 2011; 6:e16332. [PubMed: 21298110]
15. Cai C, Hsieh C, Omwancha J, Zheng Z, Chen S, Baert J, Shemshedini L. ETV1 is a novel androgen receptor-regulated gene that mediates prostate cancer cell invasion. Mol Endocrinol. 2007; 21:1835–46. [PubMed: 17505060]
16. Skehan P, Storeng R, Scudiero D, Monks A, McMahon J, Vistica D, Warren J, Bokesch H, Kenney S, Boyd M. New colorimetric cytotoxicity assay for anticancer-drug screening. J Natl Cancer Inst. 1990; 82:1107–12. [PubMed: 2359136]
17. Munker R, Kobayashi T, Elstner E, Norman A, Uskokovic M, Zhang W, Andreeff M, Koeffler H. A new series of vitamin D analogs is highly active for clonal inhibition, differentiation, and induction of WAF1 in myeloid leukemia. Blood. 1996; 88:2201–9. [PubMed: 8822940]
18. O'Kelly J, Uskokovic M, Lemp N, Vadgama J, Koeffler H. Novel Gemini-vitamin D3 analog inhibits tumor cell growth and modulates the Akt/mTOR signaling pathway. J Steroid Biochem Mol Biol. 2006; 100:107–16. [PubMed: 16777406]
19. Thoennissen N, Iwanski G, Doan N, Okamoto R, Lin P, Abbassi S, Song J, Yin D, Toh M, Xie W, Said J, Koeffler H. Cucurbitacin B induces apoptosis by inhibition of the JAK/STAT pathway and potentiates antiproliferative effects of gemcitabine on pancreatic cancer cells. Cancer Res. 2009; 69:5876–84. [PubMed: 19605406]
20. Rostad K, Mannelqvist M, Halvorsen OJ, Oyan AM, Bø TH, Stordrange L, Olsen S, Haukaas SA, Lin B, Hood L, Jonassen I, Akslen LA, et al. ERG upregulation and related ETS transcription factors in prostate cancer. Int J Oncol. 2007; 30:19–32. [PubMed: 17143509]

21. Tomlins S, Laxman B, Dhanasekaran S, Helgeson B, Cao X, Morris D, Menon A, Jing X, Cao Q, Han B, Yu J, Wang L, et al. Distinct classes of chromosomal rearrangements create oncogenic ETS gene fusions in prostate cancer. Nature. 2007; 448:595–9. [PubMed: 17671502]
22. Ikezoe T, Gery S, Yin D, O'Kelly J, Binderup L, Lemp N, Taguchi H, Koeffler H. CCAAT/enhancer-binding protein delta: a molecular target of 1,25-dihydroxyvitamin D3 in androgen-responsive prostate cancer LNCaP cells. Cancer Res. 2005; 65:4762–8. [PubMed: 15930295]
23. Vegesna V, O'Kelly J, Said J, Uskokovic M, Binderup L, Koeffle HP. Ability of potent vitamin D3 analogs to inhibit growth of prostate cancer cells in vivo. Anticancer Res. 2003; 23:283–9. [PubMed: 12680225]
24. Verlinden L, Verstuyf A, Quack M, Van Camp M, Van Etten E, De Clercq P, Vandewalle M, Carlberg C, Bouillon R. Interaction of two novel 14-epivitamin D3 analogs with vitamin D3 receptor-retinoid X receptor heterodimers on vitamin D3 responsive elements. J Bone Miner Res. 2001; 16:625–38. [PubMed: 11315990]
25. Eelen G, Verlinden L, Rochel N, Claessens F, De Clercq P, Vandewalle M, Tocchini-Valentini G, Moras D, Bouillon R, Verstuyf A. Superagonistic action of 14-epi-analogs of 1,25-dihydroxyvitamin D explained by vitamin D receptor-coactivator interaction. Mol Pharmacol. 2005; 67:1566–73. [PubMed: 15728261]
26. Olivera CJ, Bula CM, Bishop JE, Adorini L, Manchand P, Uskokovic MR, Norman AW. Characterization of five 19-nor-analogs of 1alpha,25(OH)2-Vitamin D3 with 20-cyclopropyl-modified side-chains: implications for ligand binding and calcemic properties. J Steroid Biochem Mol Biol. 2004; 89–90:99–106.
27. Muindi JR, Modzelewski RA, Peng Y, Trump DL, Johnson CS. Pharmacokinetics of 1alpha,25-dihydroxyvitamin D3 in normal mice after systemic exposure to effective and safe antitumor doses. Oncology. 2004; 66:62–6. [PubMed: 15031600]
28. Papapoulos SE, Clemens TL, Sandler LM, Fraher LJ, Winer J, O'Riordan JL. The effect of renal function on changes in circulating concentrations of 1,25-dihydroxycholecalciferol after an oral dose. Clin Sci (Lond). 1982; 62:427–9. [PubMed: 6896025]
29. Thorne JL, Maguire O, Doig CL, Battaglia S, Fehr L, Sucheston LE, Heinaniemi M, O'Neill LP, McCabe CJ, Turner BM, Carlberg C, Campbell MJ. Epigenetic control of a VDR-governed feed-forward loop that regulates p21(waf1/cip1) expression and function in non-malignant prostate cells. Nucleic Acids Res. 2011; 39:2045–56. [PubMed: 21088000]
30. Mochizuki T, Kitanaka C, Noguchi K, Muramatsu T, Asai A, Kuchino Y. Physical and functional interactions between Pim-1 kinase and Cdc25A phosphatase. Implications for the Pim-1-mediated activation of the c-Myc signaling pathway. J Biol Chem. 1999; 274:18659–66. [PubMed: 10373478]
31. Bachmann M, Hennemann H, Xing P, Hoffmann I, Möröy T. The oncogenic serine/threonine kinase Pim-1 phosphorylates and inhibits the activity of Cdc25C-associated kinase 1 (C-TAK1): a novel role for Pim-1 at the G2/M cell cycle checkpoint. J Biol Chem. 2004; 279:48319–28. [PubMed: 15319445]
32. Wang Z, Bhattacharya N, Mixter P, Wei W, Sedivy J, Magnuson N. Phosphorylation of the cell cycle inhibitor p21Cip1/WAF1 by Pim-1 kinase. Biochim Biophys Acta. 2002; 1593:45–55. [PubMed: 12431783]

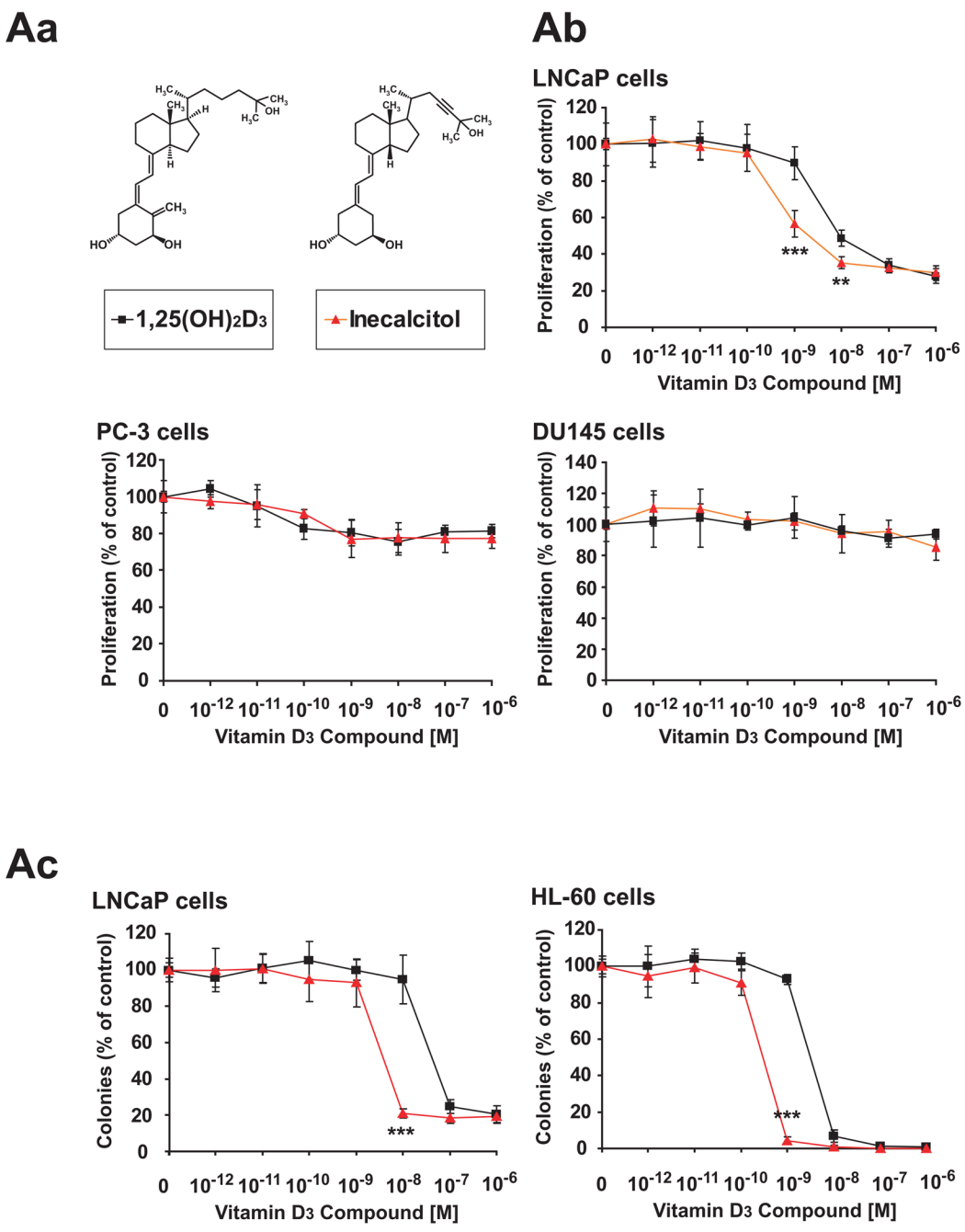

Fig. 1. Chemical structures of vitamin D_3 compounds and their effect on proliferation of cancer cells

(Aa) Chemical structures of vitamin D_3 compounds. **(Ab)** Dose–response effects of vitamin D_3 compounds on proliferation of cancer cell lines. SRB assay measuring proliferation of LNCaP, PC-3 and DU145 (prostate) cell lines at 120 h. **(Ac)** Clonal proliferation of either LNCaP or HL-60 (leukemia) cells treated with varying doses of either $1,25(OH)_2D_3$ or inecalcitol for 10–14 days. ED_{50s} are listed in Supplemental Table 2. **, $p<0.01$; ***, $p<0.001$; ■, $1,25(OH)_2D_3$; ▲, Inecalcitol.

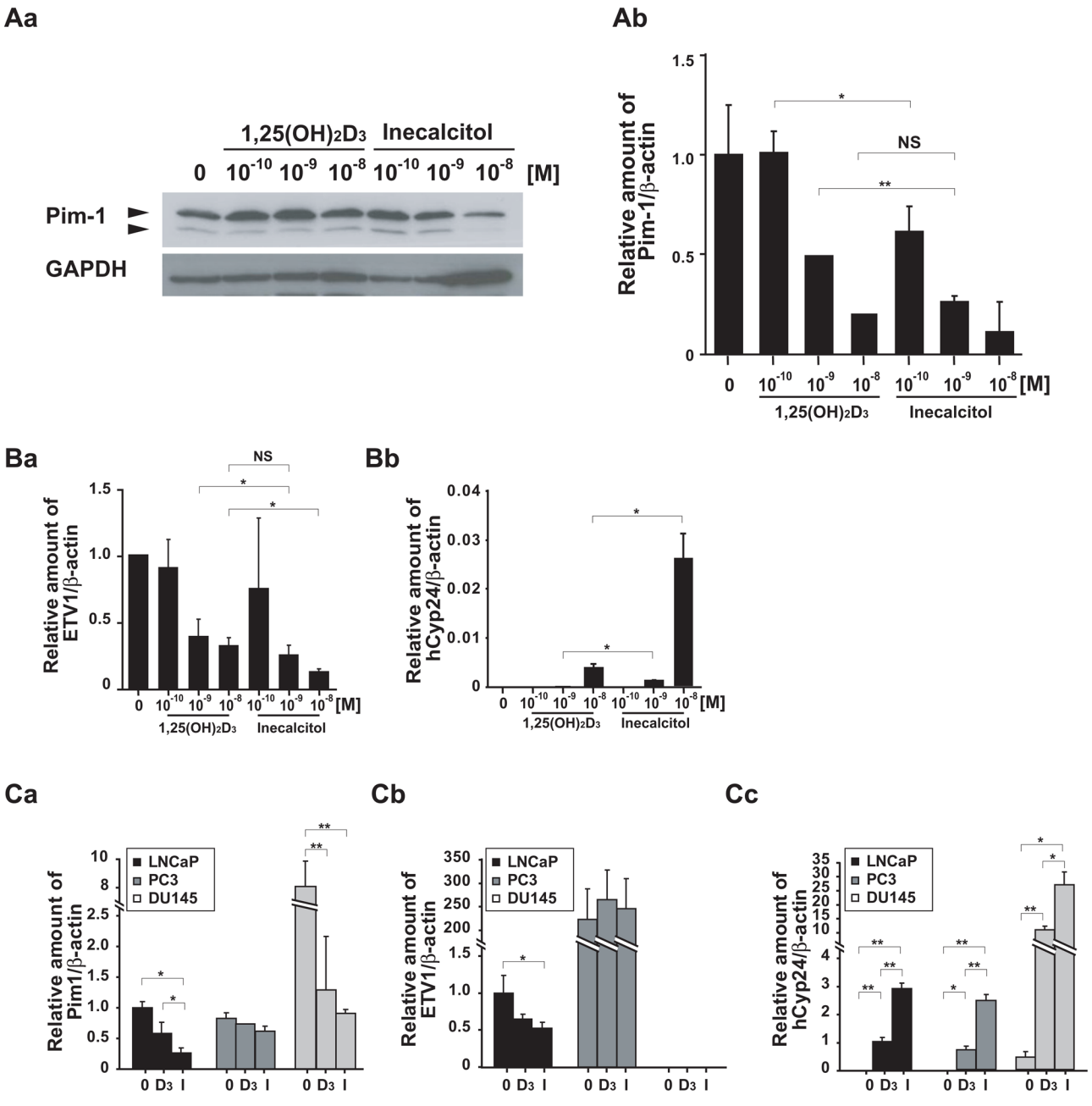

Fig. 2. Effects of vitamin D_3 compounds on gene expression

(A) Treatment with vitamin D_3 compounds inhibits levels of Pim-1. LNCaP cells were treated with 10^{-10} to 10^{-8} M of either $1,25(OH)_2D_3$ or inecalcitol for 48 h. **(Aa)** Pim-1 protein levels were analyzed by Western blot. **(Ab)** Pim-1 mRNA levels were measured by qRT-PCR, and the expression levels were normalized with β-actin. **(B)** Treatment with vitamin D_3 compounds modulates genes expression in a dose-dependent manner. LNCaP cells were treated with 10^{-10} to 10^{-8} M of either $1,25(OH)_2D_3$ or inecalcitol for 48 h. The mRNA expression levels of **(Ba)** ETV1 and **(Bb)** human Cyp24 (hCyp24) were measured by qRT-PCR, and the levels were normalized with β-actin. **(C)** Comparison of gene expression pattern in LNCaP, PC-3 and DU145 cell lines. The cells were treated with 10^{-8} M of either $1,25(OH)_2D_3$ or inecalcitol for 48 h and mRNA expression of **(Ca)** Pim-1, **(Cb)** ETV1 and

(Cc) hCyp24, as well as, β-actin were quantitated by qRT-PCR. The results are normalized to β-actin levels, and displayed as means and SDs of triplicates. *, $p<0.05$; **, $p<0.01$; NS, no significant difference; 0, Control; D_3, $1,25(OH)_2D_3$; I, inecalcitol treatment.

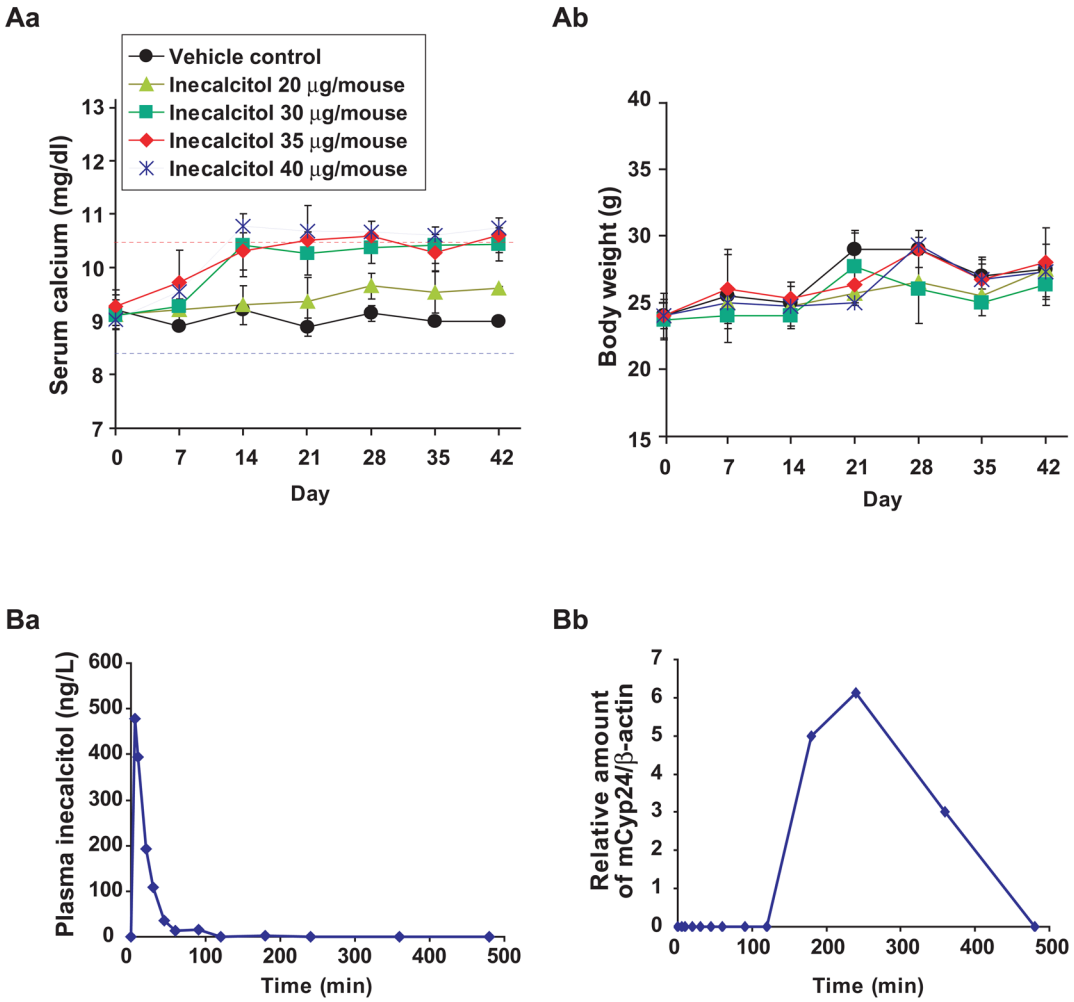

Fig. 3. ***In vivo*** **administration of inecalcitol: serum calcium, body weights, plasma half-life and Cyp24 levels**

(A) C57BL/6J mice received 20 – 40 μg of inecalcitol three times per week by i.p. for 6 weeks, and serum calcium levels were measured once a week and presented as means and SDs. **(Aa)** Overall serum calcium levels and **(Ab)** body weights of the treated mice. ●, vehicle control; ▲, 20;■, 30; ◆, 35; *, 40 μg/mouse of inecalcitol. The MTD (normal calcemic) of inecalcitol by i.p. was 30 μg/mouse (1,300 μg/kg). **(B)** Pharmacokinetics of inecalcitol in mice (N=3). **(Ba)** Plots of plasma concentration of inecalcitol and **(Bb)** mouse Cyp24 (mCyp24) mRNAlevels in liver were measured at indicated time points after injection of inecalcitol (1,300 μg/kg/mouse, i.p.). The results are presented as means (N=3). Plasma calcium levels were in normal range (data not shown) throughout the experiments. Pharmacokinetic studies showed that plasma half-life of inecalcitol was 18.3 minutes. Other pharmacokinetic data are listed in Supplemental Table 3

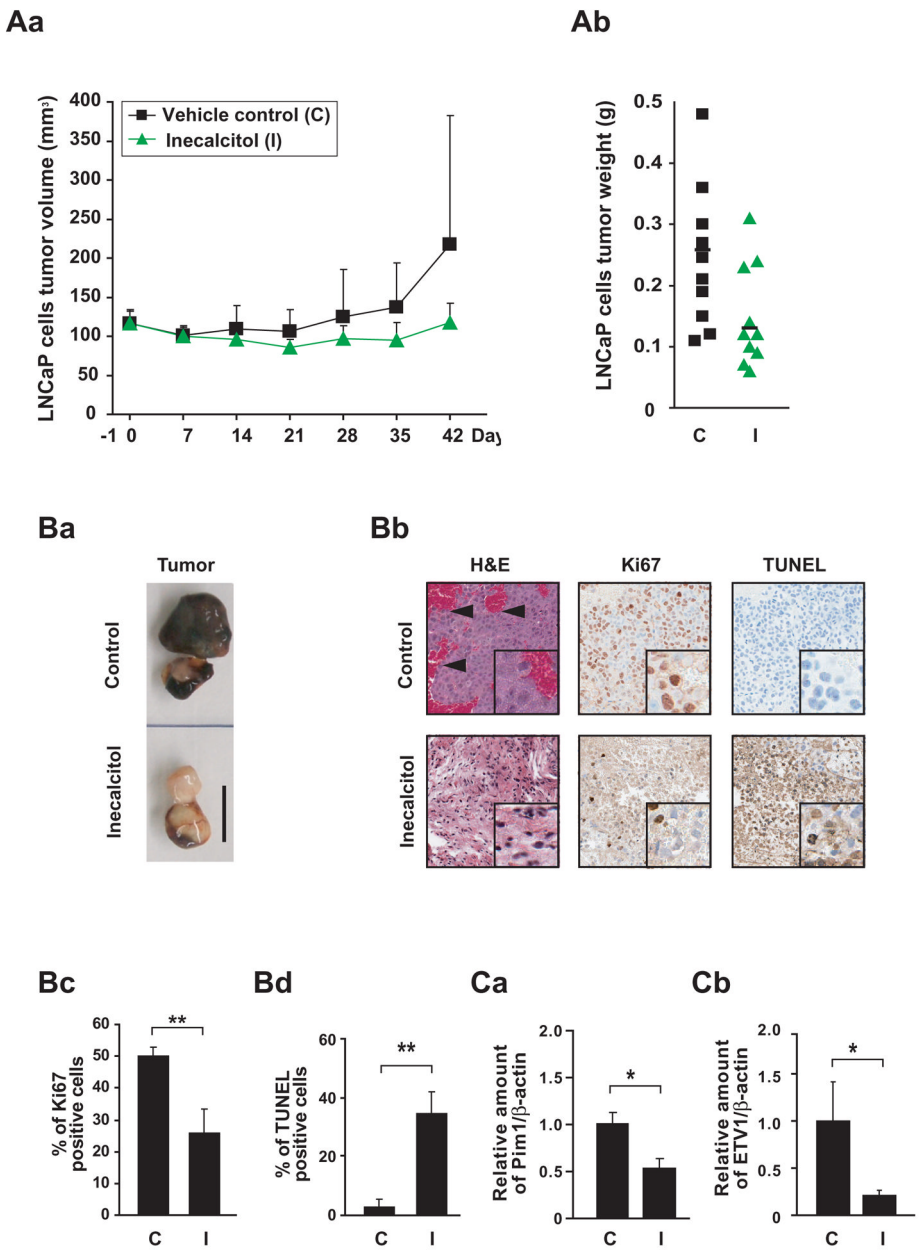

Fig. 4. Inecalcitol treatment: LNCaP human prostate tumor xenografts in a murine model system

LNCaP cells (1×10^7) were subcutaneously implanted into both flanks of BNX mice (two tumors per mouse). Inecalcitol was given three times per week for 42 days. Murine groups: C, vehicle control (N=5); I, treatment with 1,300 μg/kg of inecalcitol (N=5). *, $p<0.05$; **, $p<0.01$ **(Aa)** Overall volume of tumors. Tumor volumes were assessed by vernier calipers and presented as means and SDs. **(Ab)** Weights of dissected tumors at day 42. **(Ba)** Representative dissected tumors; note dark color of control tumors as a result of extensive vascularity. (**Bb**) Representative H&E, Ki67 and TUNEL staining of dissected tumors. Arrowhead, blood islands in the tumor; small box, magnified picture. The percent of Ki67 positive cells (**Bc**) and TUNEL positive cells (**Bd**) were quantified from the stained slides.

(Ca) Pim-1 and **(Cb)** ETV1 mRNA expression levels in the tumors at day 42 were quantitated by qRT-PCR (mean of three tumors).